Adsorption of a random copolymer at a lipid bilayer membrane

Aleksander V. Ermoshkin,[1] Jeff Z. Y. Chen,[1,2,*] and Pik-Yin Lai[2,3]
[1]*Department of Physics, University of Waterloo, Waterloo, Ontario, Canada N2L 3G1*
[2]*Physics Division, National Center of Theoretical Science, P.O. Box 2-131, Hsinchu, Taiwan 300, Republic of China*
[3]*Department of Physics and Center for Complex Systems, National Central University, Chung-Li, Taiwan 320, Republic of China*
(Received 14 May 2002; published 21 November 2002)

We examine the conformational properties of a random copolymer, containing a disordered hydrophobic/hydrophilic sequence of monomers, in the presence of a hydrophobic potential well. The model can be used to understand the structural properties of the adsorption of a protein molecule at a lipid-bilayer membrane, and the properties of a random copolymer at the surfaces of a microphase-separated layered polymer structure. Using a trial-potential treatment we demonstrate that a mainly hydrophilic chain may localize on the surface of the bilayer and that a mainly hydrophobic chain may have two typical conformations: localization on the surface or complete adsorption inside the two surfaces.

DOI: 10.1103/PhysRevE.66.051912 PACS number(s): 87.15.Aa, 61.41.+e, 87.14.Ee

I. INTRODUCTION

The interest in the physical properties of a model polymer chain containing two types of monomers *A* and *B* at an interface stems from attempts at understanding practical systems that contain proteins and random copolymers. In particular, recent attention has been focused on the behavior of a random copolymer at a flat interface between two immiscible solvents, one preferring *A* and the other *B* [1,2]. In addition to the practical usefulness of this model system, the unusual localization phenomenon expected in this type of system [3] has also inspired active theoretical studies in recent years [4–21].

Protein molecules are known to contain a disordered sequence of hydrophobic and hydrophilic residues, which in a simplified version can be considered as random copolymer (RCP). The binding of a membrane protein to a lipid bilayer largely depends on the competition between the hydrophobicity of each monomer and the resulting conformational entropy of an adsorbed protein. It is commonly understood that, since the interior of a lipid bilayer is hydrophobic, an entirely hydrophilic chain cannot bind to the lipid bilayer. However, less obvious is the possibility that a mainly hydrophilic chain containing some hydrophobic monomers may become *localized* at the lipid layer/water interface. Here we use the terminology ''adsorption'' and ''localization'' to represent two different types of density profile. Figure 1(a) illustrates a surface-localized RCP where the gray region represents a hydrophobic environment. As long as a significant segment of hydrophobic monomers exists, that segment will attempt to locate itself inside the bilayer, despite the fact that the chain could be dominantly hydrophilic. This is in strong contrast with Fig. 1(b) where the entire chain can be *adsorbed* into the interior of the bilayer region when the chain is mainly hydrophobic.

In this paper, we aim at understanding the interplay between sequence-dependent hydrophobicity and adsorption energy using a simple model. A random copolymer chain is assumed to carry two types of monomers, *A* (hydrophobic) and *B* (hydrophilic), and the gray area in Fig. 1 energetically prefers *A* monomers with an adsorption energy gain ξ per monomer. For a fixed potential-well gap $2d$ and a weak ξ the problem can be separated into two uncorrelated interfaces, each hosting a significant portion of a localized RCP, as illustrated in Fig. 1(a). On the other hand, a strong ξ corresponds to an adsorption system of which the main portion of the polymer stays inside the potential well, as illustrated in Fig. 1(b). A crossover point exists where a mainly localized phase switches to a mainly adsorbed phase, as the physical conditions change. A phase diagram in terms of scaled variables is presented in Sec. III.

II. MODEL AND METHOD

Mathematically, we consider a polymer chain consisting of N monomers, whose spatial configuration can be denoted by $\vec{r}(s)$, and each monomer experiences an external field

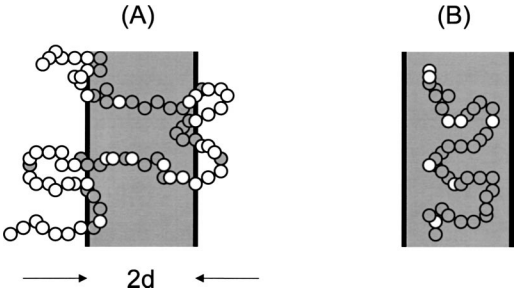

FIG. 1. Sketch of two surface conformations. A random copolymer can be in a surface-localized state (a), where the monomer density is much higher at the two interfaces, or in a completely adsorbed state (b), where the majority of monomers are located in the interior of the potential well. Here, the gray area represents a solvent environment that prefers the gray monomers. In the case where a random copolymer contains more gray monomers, there is a smooth transition from a localized state to the adsorbed state as the temperature is raised. In the case where a random copolymer contains fewer gray monomers, surface localization is still possible; the random copolymer can be delocalized as the temperature is raised.

*Corresponding author. Email address: jeffchen@uwaterloo.ca

$w(z)$ which characteristically describes the bilayer background. The potential energy that describes the interaction between monomer s and the background field $w(z)$ has the form

$$V[z(s),s]=[\xi+\epsilon(s)]w[z(s)] \tag{1}$$

where ξ is an average interaction parameter. The function $\epsilon(s)$ is a random number that depends on the sequence,

$$\langle \epsilon(s)\rangle = 0, \tag{2}$$

$$\langle \epsilon(s)\epsilon(s')\rangle = \Delta^2 \delta(s-s'), \tag{3}$$

where $\delta(s)$ is Dirac's delta function. The angular brackets in the above expressions represent an average over the sequence distribution. Δ is a characteristic parameter measuring the strength of the disorderedness. The external potential $w(z)$ is assumed to have the form

$$w(z)=\begin{cases} -1, & |z|<d, \\ 1, & |z|>d, \end{cases} \tag{4}$$

where the width of the potential well is $2d$. For a chain containing mainly hydrophobic monomers, $\xi>0$, and conversely for a chain containing mainly hydrophilic monomers, $\xi<0$.

The partition function of the chain can be written in terms of a functional integral,

$$Q=\int D[z(s)]\exp\left(-\int_0^N\left[\frac{D}{2a^2}\left(\frac{dz}{ds}\right)^2+\beta V[z(s),s]\right]ds\right) \tag{5}$$

where $z(s)$ is the z-direction coordinate of the sth monomer, $D=3$ the dimensionality of space, and $\beta=1/k_BT$ the inverse temperature. Introducing a trial potential $v(z)$ we have [19]

$$Q=\int D[z(s)]\exp\{-H_0[z(s)]-H_1[z(s)]\} \tag{6}$$

with functionals

$$H_0[z(s)]=\int_0^N\left\{\frac{D}{2a^2}\left(\frac{dz}{ds}\right)^2+\beta\xi w(z(s))+v(z(s))\right\}ds \tag{7}$$

and

$$H_1[z(s)]=\int_0^N\{\beta\epsilon(s)w(z(s))-v(z(s))\}ds. \tag{8}$$

The main purpose of the introduction of a sequence-independent trial potential $v(z)$ is to enable the calculation of the conformational properties in terms of a simple form of $v(z)$. Performing the disorderedness average $\langle\cdots\rangle$ we have

$$\langle F\rangle = F_0+\langle\overline{H_1}\rangle-\frac{1}{2}(\langle\overline{H_1^2}\rangle-\langle\overline{H_1}^2\rangle)+\cdots \tag{9}$$

where F_0 is the free energy associated with the unperturbed Hamiltonian H_0. The overbar in Eq. (9) represents an ensemble average in the configurational space with respect to the Boltzmann factor of H_0. We adjust the potential $v(z)$ so that the terms involving the disorder average in Eq. (9) cancel each other and hence we can adopt the free energy F_0 as an approximation for F. This produces a matching condition

$$\overline{v}=-\frac{1}{2}(\beta\Delta)^2(\overline{w^2}-\overline{w}^2)+O[(\beta\Delta)^4] \tag{10}$$

where

$$\begin{aligned} v[z(s)]&=-\int_0^N v(z(s))ds, \\ w[z(s)]&=-\int_0^N w(z(s))ds, \\ w^2[z(s)]&=-\int_0^N [w(z(s))]^2 ds. \end{aligned} \tag{11}$$

Equation (9) is a free-energy expansion in powers of disorder. By truncating the expansion we are actually considering a perturbation approach. Dropping higher order terms in Eq. (9) is effectively dropping terms of order $(\beta\Delta)^4$ as displayed in Eq. (10). Strictly speaking this approximation is valid in the high-temperature, low-disorder limit.

We are interested in the long polymer limit only ($N\gg 1$). In this limit, the ground-state dominance approximation [22] relates the solution $\Psi(z)$ of a stationary Schrödinger equation

$$\left(-\frac{a^2}{2D}\nabla^2+\beta\xi w(z)+v(z)\right)\Psi(z)=E\Psi(z) \tag{12}$$

to the monomer density distribution function of the system $\rho(z)=\Psi(z)^2$. In the long chain limit, the free energy per monomer, f, is simply related to the eigenenergy E by $\beta f=E$ [22].

With the assumption that the localization potential at both $z=d$ and $z=-d$ can be represented by a δ function,

$$v(z)=-v_0\delta(|z|-d), \tag{13}$$

where $v_0>0$ is an adjustable parameter used in the matching condition Eq. (10), we are able to analytically solve Eq. (12). At the level of ground-state-dominating approximation, we can show that the free-energy minimum corresponds to an even density profile, for which the wave function has the form

$$\Psi(z)=\begin{cases} A_1\cosh(k_1z), & |z|<d, \\ A_2\exp(-k_2|z|), & |z|>d, \end{cases} \tag{14}$$

where A_1, A_2, k_1, k_2 are the wave function parameters. These parameters can be determined by equating the wave function at $z=\pm d$, considering the mismatch of the slope of the wave function at $z=\pm d$ caused by the δ function poten-

tial, and normalizing the monomer density function. This procedure yields a set of algebraic equations that relate the parameters,

$$-\frac{a^2}{2D}k_1^2-\beta\xi=E, \tag{15}$$

$$-\frac{a^2}{2D}k_2^2+\beta\xi=E, \tag{16}$$

$$A_1\cosh(k_1d)=A_2\exp(-k_2d), \tag{17}$$

$$v_0=\frac{a^2}{2}[k_1\tanh(k_1d)+k_2], \tag{18}$$

and

$$A_1^2\left(\frac{\sinh(2k_1d)}{2k_1}+d\right)+A_2^2\frac{\exp(-2k_2d)}{k_2}=1. \tag{19}$$

Evaluating the averages in Eq. (11) and substituting them into Eq. (10) with the help of Eqs. (17) and (19) we get

$$v_0=(\beta\Delta)^2\left(k_1\frac{\cosh(2k_1d)+1}{\sinh(2k_1d)+2k_1d}+k_2\right)^{-1}. \tag{20}$$

The last six equations completely determine the six parameters A_1, A_2, k_1, k_2, v_0, and E, and hence completely determine the physical properties of the system. These six equations also contain the reduced inverse temperature $\beta\Delta$ as an essential system-dependent parameter.

III. RESULTS AND DISCUSSION

The introduction of scaled parameters

$$\overline{k}_{1,2}=\frac{a}{\sqrt{2D}\beta\Delta}k_{1,2}, \tag{21}$$

$$\overline{d}=\frac{\sqrt{2D}\beta\Delta}{a}d, \tag{22}$$

$$\overline{\xi}=\frac{2}{\beta\Delta^2}\xi \tag{23}$$

eliminates the $\beta\Delta$ dependence in the last six equations. In addition to the mathematical convenience in a reduced form, Eqs. (21)–(23) provide deeper physical insights. According to Eq. (21), any physical property associated with a length L has the scaling form

$$L=(a/\beta\Delta)G_1(\beta\Delta d/a,\xi/\beta\Delta^2). \tag{24}$$

In addition, the free energy of the system $f\equiv E/\beta$ scales as

$$f=(\beta\Delta^2)G_2(\beta\Delta d/a,\xi/\beta\Delta^2). \tag{25}$$

Here, both G_1 and G_2 are dimensionless functions. One conclusion that we can immediately draw is the scaling behavior of the critical inverse temperature for the desorption transition, which can be determined by letting $f=f_{\text{bulk}}=\xi$,

$$\beta_c\Delta=(\xi/\Delta)G_3(\beta\Delta d/a). \tag{26}$$

This equation, in the limit $d\gg a/\beta\Delta$, gives a critical inverse temperature directly proportional to $|\xi|/\Delta^2$. In this case, the two interfaces are very far from each other and can be viewed effectively as two uncorrelated interfaces. For a negative ξ, the regions on the left and right sides are energetically preferred; thus the RCP delocalizes and move to one of these regions. This scaling relation is identical to the critical point determined earlier in Refs. [3] and [19].

Combining Eq. (15) with Eq. (16) and Eq. (18) with Eq. (20) we have

$$\overline{k}_2^2-\overline{k}_1^2=\overline{\xi}, \tag{27}$$

$$\overline{k}_1f_1(\overline{k}_1\overline{d})+\overline{k}_2=[\overline{k}_1f_2(2\overline{k}_1\overline{d})+\overline{k}_2]^{-1}, \tag{28}$$

where the functions $f_1(x)$ and $f_2(x)$ are given by

$$f_1(x)=\tanh(x), \tag{29}$$

$$f_2(x)=\frac{\cosh(x)+1}{\sinh(x)+x}. \tag{30}$$

The solution of Eqs. (27) and (28) further determines the conformational properties of the system.

We note that $\overline{k}_2$ is always real and positive; however, $\overline{k}_1$ can be real or imaginary depending on the values of $\overline{\xi}$ and d. In the case of a real $\overline{k}_1$, Eq. (27) represents a hyperbola defined on a $(\overline{k}_1,\overline{k}_2)$ plane for both positive and negative $\overline{\xi}$. In the case of imaginary $\overline{k}_1$ this equation represents a circle and the values of $\overline{\xi}$ can only be positive.

First we consider a positive $\overline{\xi}$ where the interior of the potential well is preferred by the RCP. In the transmembrane protein case this means that the entire chain is hydrophobic on average. Two asymptotic limits corresponding to known results can be recovered from our calculation. In the case of $\overline{\xi}\ll 1$, there is no net energetic gain for the RCP to be adsorbed inside the potential well. However, due to disorderedness in the sequence, the RCP can be localized at the two interfaces. The density profile can be schematically represented by Fig. 2(a), where the density decays outside the potential well exponentially as has been discussed before [17,19] and the density profile inside the well displays a squared hyperbolic cosine function. More importantly, in the entire range of the reduced variable $\beta\Delta d/a$, the free energy is proportional to $\beta\Delta^2$, which is a signature of RCP localization [3]. Another asymptotic limit is the case of $\overline{\xi}\gg 1$. Since the adsorption preference is so large, the localization phenomenon is completely hidden. The typical density profile is represented in Fig. 2(b). Now, the free energy per monomer can be estimated to have the magnitude $-\overline{\xi}$, which is simply equal to the energy gain for each monomer to be adsorbed inside the potential well.

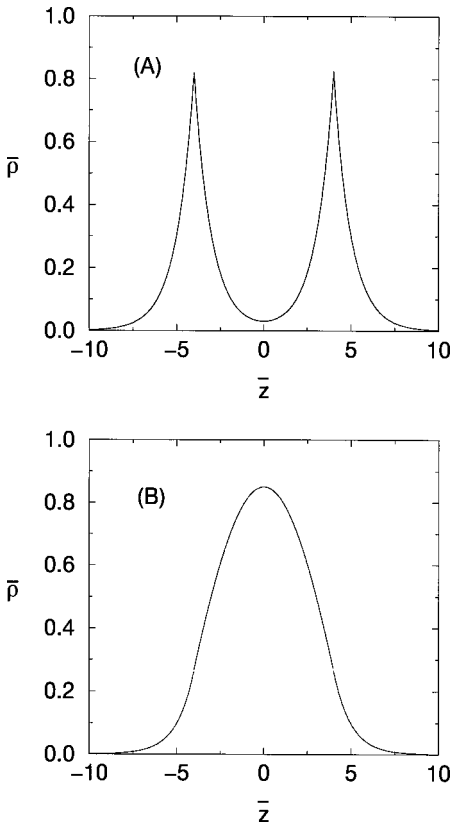

FIG. 2. Typical monomer density profiles. In a localized state (a), the monomer density is more concentrated near the interfacial areas and the interior of the potential well/barrier has less monomers except for occasional crossing of polymer segments [see Fig. 1(a)]. In an adsorbed state (b), the monomer density is significant only in the central region of the potential well.

More precise information can be gained from solving Eqs. (27) and (28). Typical geometrical representations of Eqs. (27) and (28) are shown in Fig. 3 where the intersections give the solutions to these two equations. For small and positive $\bar{\xi}$ (attractive potential well) Eq. (27) represents branches of a hyperbola pointing upright with a minimum located at $\bar{k}_1=0$, $\bar{k}_2=\sqrt{\bar{\xi}}$. Equation (28) is also symmetric about $\bar{k}_1=0$ and has a maximum $\bar{\xi}_{\rm cr}^{1/2}$ on the $(\bar{k}_1,\bar{k}_2)$ plane. Since both $\bar{k}_1$ and $\bar{k}_2$ are real, the typical density profile has two peaks located at the two interface boundaries [Fig. 2(a)].

As we increase $\bar{\xi}$ (increasing well depth) the hyperbola starts to move up and as $\bar{\xi}$ reaches the value $\bar{\xi}_{\rm cr}$ the real solution for $\bar{k}_1$ and $\bar{k}_2$ disappears. Hence, we need to consider an imaginary $\bar{k}_1$ and switch to the situation shown in Fig. 3(b). In this case Eq. (27) represents a circle which intersects the curve given by Eq. (28) for any $\bar{\xi}>\bar{\xi}_{\rm cr}$. A typical monomer density profile for an imaginary $\bar{k}_1$ is shown in Fig. 2(b) and corresponds to a chain totally adsorbed to the interior of an attractive potential well.

The transition between these two key types of density profile, localized and adsorbed, takes place at

$$\bar{k}_1=0. \tag{31}$$

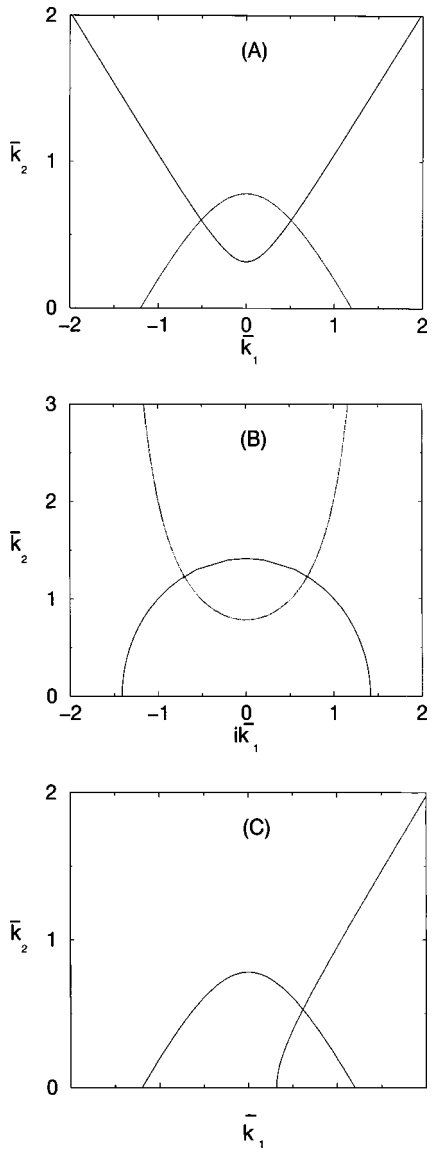

FIG. 3. Schematic illustration of the solution to Eqs. (27) and (28) in terms of intersections of curves on the $\bar{k}_1$ and $\bar{k}_2$ plane. In plots (a) and (c), both $\bar{k}_1$ and $\bar{k}_2$ are real numbers. In plot (b) $\bar{k}_2$ is real whereas $\bar{k}_1$ is imaginary.

This transition curve, in terms of $\bar{\xi}$ and $\bar{d}$, can be directly determined from Eqs. (27) and (28) and is the solution of

$$\bar{\xi}+\sqrt{\bar{\xi}}/\bar{d}-1=0.$$

The dashed curve in Fig. 4 demonstrates the localization-adsorption transition. Due to the analytical nature of the functions involved in determining this transition, in particular, the analytical transition between real $\bar{k}_1$ and imaginary $\bar{k}_1$, no mathematical singularity in the thermodynamical properties is observed near the transition, which rules out the possibility of associating this crossover phenomenon with a phase transition.

One surprising consequence of this analysis is that the transition from an adsorbed state to a localized state is pos-

sible as the temperature *decreases* for fixed ξ and d. This is particularly relevant to a transmembrane protein system, where both the average hydrophobicity for a given protein and the width of the lipid bilayer are fixed. A change in the reduced $\bar{\xi} \propto \xi/\beta\Delta^2$ and $\bar{d} \propto \beta\Delta d$ is possible through changing temperature. In an adsorbed state, a characteristic free energy per monomer is $-\xi$ at low temperature while in a localized state the free energy per monomer can be estimated to have the order $-\beta\Delta^2$.

Secondly, we consider the case of $\xi<0$, for which the gray region in Fig. 1 actually represents a net repulsive barrier. This corresponds to the case of a mainly hydrophilic chain, whose average interaction with the interior of a lipid membrane is repulsive. Because of the lower energies outside the potential barrier, a homopolymer with $\xi<0$ cannot be adsorbed in any region near the barrier. However, a localized RCP takes advantage of the presence of interfaces and can still localize at the two interfacial boundaries at appropriate temperatures. Mathematically, the branches of the hyperbola describing Eq. (27) point in the right direction [see Fig. 3(c)]. Only a real $\bar{k}_1$ solution is possible, which corresponds to the boundary localized state shown in Fig. 2(a).

The localized RCP, however, is subject to a repulsive interaction with the solvent inside the potential barrier, and will leave the interfaces when the localization free-energy gain is less than the net repulsive potential energy. This transition is determined by the fact that the solution to the coupled Eqs. (27) and (28) disappears as $\bar{\xi}$ reaches $\bar{\xi}_{\rm tr}$. The transition line is analytically determined by letting $\bar{k}_2=0$, which is equivalent to the statement that the free energy reaches a value equal to that in the bulk region (the region far from the interfaces): $f=\beta\xi$. The solid curve in Fig. 4 represents this phase boundary. We can further show that this localization-delocalization transition has the characteristics of a second order phase transition, at least based on the current trial-function treatment. Monthus has demonstrated for a similar system that this transition could be of a different type based on her renormalization treatment [18].

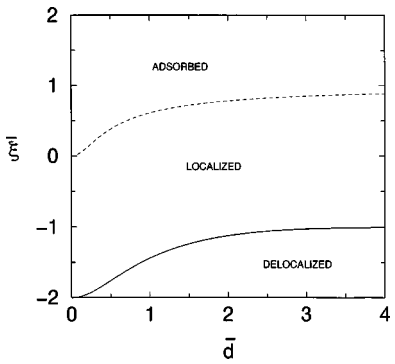

FIG. 4. Phase diagram of a random copolymer chain in terms of reduced system parameters $\bar{d}=\sqrt{6}\beta\Delta d/a$ and $\bar{\xi}=2\xi/\beta\Delta^2$. The solid curve represents a delocalization-localization transition of the characteristics of a second order phase transition, and the dotted curve represents a crossover from the adsorbed state to a localization state. Crossing of these phase boundaries is possible by changing the temperature (see text).

IV. CONCLUDING REMARKS

In summary, we have carried out a calculation of the phase diagram for a random copolymer located near a potential well/barrier, based on a trial-function approach developed earlier by one of us [19]. The system may display delocalization/localization/adsorption states depending on two reduced parameters $k_BT\xi/\Delta^2$ and $d\Delta/(k_BTa)$. In a protein system, ξ is the average interaction parameter with the hydrophobic environment in the lipid bilayer, Δ the variation of hydrophobicity along the protein chain, and d the half width of the lipid bilayer.

Two important features emerges from our study. Using the language of protein adsorption, we have demonstrated that a mainly hydrophobic protein chain ($\xi>0$) can always be adsorbed to the lipid bilayer system; however, it may display different conformational properties. At low temperatures, the monomers are more concentrated near the two bilayer surfaces than in the central region, and at high temperatures, the monomers are more concentrated near the center of the bilayer. The characteristic free energies of these two states are different; the former is proportional to $-\beta\Delta^2$ and the latter to $-\xi$. A smooth transition from the localized state to the adsorbed state is possible as T increases.

Another important but yet counterintuitive feature is the possibility of localization of a mainly hydrophilic chain ($\xi<0$) at the surface of the membrane. Energetically, without consideration of the entropic effect, this localization can be viewed as a perfect arrangement of the protein chain across the interfaces, such that the hydrophobic monomers are all inside and the hydrophilic monomers are all outside the lipid bilayer. At a finite temperature, the competition of this localization energy with entropy yields a delocalization transition at a temperature determined jointly by the bilayer width, the disorderedness in the chain, and the average hydrophobicity of the chain.

The trial-function approach used in this study, although very efficient, may suffer in the low-temperature region, as we have ignored any contributions of order $(\beta\Delta)^4$ in a treatment accurate to order $(\beta\Delta)^2$. In particular, since the crossover between localization and adsorption relies on an estimate of the free energy per monomer, a more accurate calculation of the free energy is desirable at low temperature. A computer simulation that solves the Schrödinger equation directly with a simulated disordered sequence [17], for example, can be useful in determining the transition from a localized state to an adsorbed state as the temperature increases.

Our main purpose is to demonstrate the effect of sequence disorderedness on the transmembrane structures using a simplified physical picture that contains only a few basic parameters. The model needs to be refined to include further complications in a real membrane system. There are other entropic/energetic contributions such as the excluded-volume interaction that are not addressed here, and may dramatically change the physical picture. For example, one needs to ad-

dress the effects that hydrophobic parts tend to occupy a space inside membrane bilayer, where due to the hydrogen bonding they form helical structures. Hydrophilic parts prefer to stay outside the membrane bilayer, where they form coil-like conformations. Internal helices can aggregate with each other forming a more compact intramembrane structure due to a van der Waals attraction.

ACKNOWLEDGMENTS

Financial support of this work was provided by NATO (A.E) and the Natural Science and Engineering Research Council of Canada (J.Z.Y.C.). J.Z.Y.C. acknowledges the hospitality of the National Central University (Taiwan) during the preparation of this manuscript.

[1] P. Chen, S. Lahooti, Z. Policova, M. A. Cabrerizo-Vilchez, and A. W. Neumann, Colloids Surf. B **6**, 279 (1996).
[2] C.-A. Dai, B. J. Dair, K. H. Dai, C. K. Ober, E. J. Kramer, C.-Y. Hui, and L. W. Jelinski, Phys. Rev. Lett. **73**, 2472 (1994).
[3] T. Garel, D. A. Huse, S. Leibler, and H. Orland, Europhys. Lett. **8**, 9 (1989).
[4] T. Garel, L. Leibler, and H. Orland, J. Phys. II **4**, 2139 (1994).
[5] Y. Lyatskaya, D. Gersappe, N. A. Gross, and A. C. Balazs, J. Phys. Chem. **100**, 1449 (1996).
[6] J.-U. Sommer, A. Halperin, and M. Daoud, Macromolecules **27**, 6991 (1994).
[7] J.-U. Sommer and M. Daoud, Europhys. Lett. **32**, 407 (1995).
[8] S. T. Milner and G. H. Fredrickson, Macromolecules **28**, 7953 (1995).
[9] J.-U. Sommer and M. Daoud, Phys. Rev. E **53**, 905 (1996).
[10] S. Stepanow, U. Bauerschäfer, and J.-U. Sommer, Phys. Rev. E **54**, 3899 (1996).
[11] J.-U. Sommer, G. W. Peng, and A. Blumen, J. Chem. Phys. **105**, 8376 (1996).
[12] S. Stepanow, J.-U. Sommer, and I. Ya. Erukhimovich, Phys. Rev. Lett. **81**, 4412 (1998).
[13] V. Ganesan and H. Brenner, Europhys. Lett. **46**, 43 (1999).
[14] J.-U. Sommer, Eur. Phys. J. B **10**, 537 (1999).
[15] A. Trovato and A. Maritan, Europhys. Lett. **46**, 301 (1999).
[16] A. Maritan, M. P. Riva, and A. Trovato, J. Phys. A **32**, L275 (1999).
[17] Z. Y. Chen, J. Chem. Phys. **111**, 5603 (1999).
[18] C. Monthus, Eur. Phys. J. B **13**, 111 (2000).
[19] Z. Y. Chen, J. Chem. Phys. **112**, 8665 (2000).
[20] N. A. Denesyuk and I. Ya. Erukhimovich, J. Chem. Phys. **113**, 3894 (2000).
[21] N. A. Denesyuk, J. Chem. Phys. **114**, 4696 (2001).
[22] A. Yu. Grosberg and A. R. Khokhlov, *Statistical Physics of Macromolecules* (AIP, New York, 1994).